

Design and Development of Compliant Anatomical Palmar Mechanism (CAPM) to Adaptively Reconfigure Precision/Power Grasps

Ivy Chang, Kok-Meng Lee*, *Life Fellow, IEEE*

Abstract— The design of a robotic hand incorporating a critical multi-DOF palm depends on studies of the anatomical structure of the human palm model. Shaping of this large grasping region is simplified to depend on arches formed by relative movement of the phalanges and metacarpal. Compliant Anatomic Palmar Mechanism (CAPM) replaces these arches to form an interconnected compliant structure that can be used in grasping to conform to contacting objects to augment stability. FEM is used to simulate the range of intrinsic movement of the palmar surface. Plotting these results determines the kinematic relationship by relating thumb rotation and metacarpal translation to the deformation of the palmar region.

I. INTRODUCTION

Human hands are highly dexterous and capable of executing complex tasks demanding both skillful handling and powerful grasping of an object. Traditionally, research on the human hand generally focuses on the former, relying primarily on multiple fingers with redundant muscular motors to achieve degree-of-freedom (DOF) manipulation. Therefore, conventionally the design objectives of a robotic hand are on the positioning of the fingers relative to the target object to maintain a stable grasp, and often neglect the role played functionally by the palm. The hand palm is less well understood, and as a result, its potential has been underexploited for enhancing a robotic hand. This paper presents the design criteria derived from a study on the anatomical structure of the human palm to enhance a robotic hand's functionality for tasks that require adaptability in partially unstructured environments.

The role the palmar region plays ranges from enhancing the dexterity of fingers or providing flexibility to the way researchers design hardware built into the hand itself. The palm is utilized to provide space for novel actuator arrays or other electronic components that use the motors to drive multiple fingers for compact operation [1][2][3]. Extendable, telescopic actuated soft palms are also implemented to prevent collision with sensitive sensors [4]. Additionally, designs have considered using the palm to broaden finger dexterity. A criterion to evaluate dexterity, thumb opposition (thumb opposing or touching other fingertips) in the BCL-26 robotic hand has a multi-DOF palm that rotates the thumb to achieve this [5]. RBO-Hand-2 also incorporates the

opposable thumb, including two extendable actuators in the palm. A compliant fiber-reinforced silicone transmits forces between the palm and the fingers to increase stability for power grasps or heavier loads [6]. To augment versatility in the hand and dexterity with the fingers, reconfigurable palms have altered its topological structure for an additional DOF to the thumb [7][8].

When considering the palm's contribution to grasping configuration, certain assumptions have been made during modeling to reduce the complexity of a multi-layer human palm into a mathematically tractable form. Characterizing the palm as a flat surface is an assumption some studies have rejected as an accurate interpretation of how palmar opposition increases stability in grasps. A study on palm concavity compares the effect of fixed and curved 2DOF palmar surfaces on the performance of a human hand when grasping various geometrical objects such as pyramids, cylinders, and spheres. The adaptable palm that emulates the motion of the thenar and hypothenar muscles yields improvement when studied against the fixed palm in grasping the sphere, pyramid, and small cylinder (20mm diameter) [9]; the results suggest various palmar angles in each distinguishable condition, implying inadequacy of estimating the palmar region as not only a level surface but also as a fixed curved area [2]. However, examining the results of arch shape modulation using the dorsum (posterior) part of the hand, the inner arch movement incorporates complications of intrinsic muscle and thickness variations. Some researchers assume the flat nature of the palmar region, instead actuating the active palm to translate vertically outwards to move the center of mass of the object to alter the contact location for the fingers [10]. Therefore, studies have not only been investigating the shape, but also the material and actuation considerations in the palmar region.

Studies have shown the commonly made general assumption of uniformly applied pressure from the palm; the palm adapts with various magnitudes of force depending on the grasped object geometry [11]. To account for similar non-uniform compression in the human palm, skin-like-material studies have been conducted to understand how this multi-layer matter affects the functionality of hands. Biomimetic skin structures have been developed to increase compression between objects and the contact area of the palm, leading to larger stability in a low-force grasp condition [12]. A combination of both active actuation and passive shape adaptation has been used to form a soft contact surface that envelops the object with variable stiffness, validated through grasping sample objects [13]. Other designs incorporate passive compliance in the palmar region; for example, RBO hand utilized pneumatically actuated silicone pads to shape match the contact area and the object in conjunction with

Ivy Chang is with the George W. Woodruff School of Mechanical Engineering, Georgia Institute of Technology, Atlanta, GA 30332, USA. (e-mail: ichang36@gatech.edu).

Kok-Meng. Lee is with the George W. Woodruff School of Mechanical Engineering, Georgia Institute of Technology, Atlanta, GA 30332, USA. (e-mail: kokmeng.lee@me.gatech.edu)

* Corresponding author: Kok-Meng Lee

compliant fingers [14]. Design of a gripper as a silicone pillar array within cylindrical palm changes in stiffness as the object comes in contact and deforms [15].

Prior research has led to a diverse field of assumptions in the palmar region and its material properties with the intent to achieve the highest level of anthropomorphism or broadening adaptability of grasping. Motivated by the need to take advantage of the palm’s functionality in the human hand to bridge understanding in its potential application in the robotic hand, the paper presents a systematic design methodology to streamline the design of the palmar region to make the appropriate assumptions. This paper contributes to three areas:

- Taking inspiration from the anatomy of the human hand, the *first* is a set of design criteria derived from a study on the anatomical palm structure. The findings will help understand the intrinsic movement of the palmar region relative to joints in the human hand
- The *second* is the design concept of a compliant anatomical palmar mechanism (CAPM), which concurrently conceives various types of grasps by utilizing compliant structures.
- The *third* is to employ finite element method (FEM) to conduct a kinematics study to track the deformation of the geometrically complex, large deflection, hyperelastic compliant structure

II. ANATOMICAL DESIGN METHOD

The importance of switching between two major classes of grasps on a day-to-day basis can be commonly observed by humans: precision manipulation and power grasps as illustrated in Fig. 1(a). The distinction between them has been interpreted in various ways by researchers; discerning precision handling as an intrinsic movement of the object independent of the arm and a power grip as a rigid relationship between object and hand [19]. Other definitions include describing a precision grip as pinching of the target object between flexed fingers and the thumb and a power grip as clamping of the flexed fingers and the counter pressure of the thumb and palmar region [20]. **Error! Reference source not found.** Tasks may require precision, power, or a combination of both grasps even when operating on the same target object. For example in Fig. 1(b), securing a jar lid requires the hand to adapt throughout the grasp : initially the dexterity of the fingertips is required to align the threads until the point when the palm is used to apply larger torque to secure the lid tightly [17]. Observation of the behavior of a housemaid and a machinist in a timeframe of a few hours captured the +2000 grasp changes that each professional underwent, requiring tasks that utilized major types of grasps [18]. These observations suggest that the conventional evaluation benchmark, positioning of the fingers relative to the target object to maintain a stable grasp, is necessary but not sufficient; it is not able to account for the wide range of complex activities that humans participate in daily when operating in unstructured environments where unknown external forces or requiring variable force inputs during evolving tasks may destabilize a system.

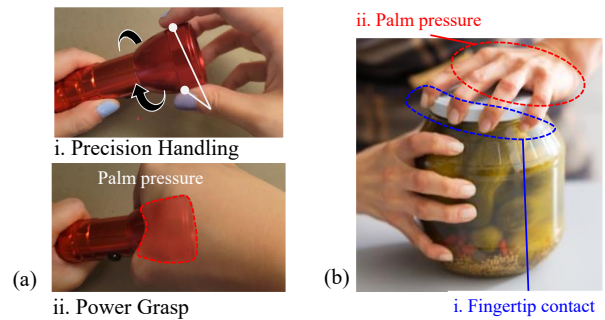


Fig. 1. Commonplace examples illustrating the role of the human palm. (a) Grasping configurations. (b) Tightening a jar lid.

Physical limitations of fixed hardware and rigid body systems can hinder the robotic hand’s ability to augment grasping capabilities in its current state. The prevalence of the palm’s use in the demonstrably versatile human hand especially in the power grasp configuration can lead to understanding its overall significance in performing various tasks. Understanding the relationship between underlying anatomical structures that produce the conforming palmar pressure contact during power grasping in humans drives the assumptions made on specific design choices for the mechanism.

Figure 2 shows breakdown of the anatomical design process employed to develop the design for the compliant palmar mechanism. The bone structure can be subdivided for the fingers (phalanges) and palm (metacarpal) in Fig. 2(a). Each phalange is composed of three components: distal, middle, and proximal which collectively are assumed equivalent in robotic finger design as rigid linkages interconnected by 1DOF rotational joints. The proximal is linked to the metacarpal head at the same position. The metacarpal is a collection of several bones which are connected at the wrist, which is defined as the robotic hand’s base. The observed relationship between the metacarpal head (MCPH) and the thumb linkage defines the palmar surface deformation seen in Fig. 2(b). Figure 2(c) illustrates the application of the design concept of the CAPM, where the metacarpal bone-segments are modeled as equivalent beams (indicated as thick black line segments) in a power grasp configuration conforming about the spherical object.

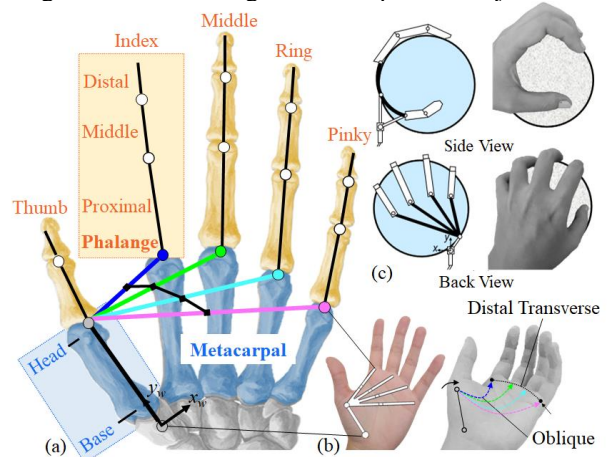


Fig. 2 CAPM based on a human hand study. (a) Schematic of the hand anatomy. (b) CAPM model based on the palm arches. (c) Power grasp demonstration.

A. Palmar Arching

Identifying two arches *oblique* and *distal transverse* that drive palmar motion, a palm arching model is developed to mechanically substitute and simulate the range of motion for the compliant mechanism, upon which the palmar region is modeled with minimum assumptions to determine the shaping as a function of a combination of rotational and translational joints.

Palmar concavity or hollowing can be described through three different curvatures: oblique, transverse, and longitudinal. The fundamental definition of arches that traverse across the human palm do not align precisely with skeletal, muscular, or other components of the human anatomy. These arches correspond to those formed by the thumb during opposition with fingers, carpal arch due to the concavity of the wrist, and carpometacarpal-phalangeal from the wrist to the corresponding metacarpal bone [21]. The distal transverse arch is formed by the concave curvature formed by the MCPH of the index, middle, ring, and little finger [22]. The two arches are driven by two fundamental types of movement in the hand: rotation of the thumb and translation of each finger's MCPH as shown in Fig. 3. Rotation of the thumb in 2DOF is defined by two angles (ζ , ψ) rotated about the wrist and the endpoint of each cantilever beam (Fig. 2c) is translated upwards in $+z$ direction by r_j for $j=1,2,3,4$ fingers. As seen in Figure 3, the rotation and translation of these joints become non-zero when shifting in grasping configuration from a flat palm to thumb opposition.

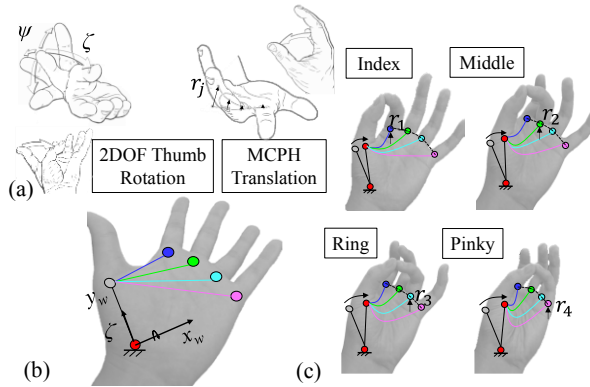


Fig. 3 Characterizing the palmar deformation (a) Oblique and distal transverse arching formed by joints. (b) Flat palm configuration (ζ , ψ , $r_j = 0$). (c) Opposition of thumb in relation to the joint parameters (ζ , ψ , $r_j \neq 0$).

B. Geometrical Model

Bioinspired soft prostheses have been created by joining together individual metacarpal bones to create the arching behavior of the hand as a means to design a biomimetic system [23]. Introducing a compliant structure to mimick the deformation of the palmar arching has the major advantage by simplifying a model of all the rigid metacarpal bones with numerous DOF. Compliance resembles the same movement while minimizing the number of moving parts to a finite set of rotational and translational joints. The arches defined in the above section are substituted with an interconnected compliant beam structure with uniform rectangular cross-section $w \times t$ ($3 \times 1.5\text{mm}$) ranging in length from the thumb MCPH to the free end of each beam l_j : 50.5, 60.5, 70.5, 75.5mm (Fig. 4). The midpoint of each beam is assumed to

be fixed as the neutral point during arching with minimal deformation. The thumb linkage connected to the wrist is rigid while the remaining structure is compliant, and made up of a hyperelastic material, such as silicone rubber. Anticipating large strain when modeling a hyperelastic, geometrically complex structure, Finite Element Method (FEM) is used to simulate deformation for a highly non-linear problem.

C. FEM Model and Curve Fitting

Compliant mechanisms have advantages over rigid bodies including but not limited to reduced friction and wear, easier manufacturing, and minimized parts [16]. However, the tradeoff involves complicated force-displacement analysis where applying classical small-deflection theory is not applicable in predicting large deflection. A FEM is set up and curve fitting is employed for non-linear properties of hyperelastic material. Curve fitting was conducted by obtaining data from Axel Products: uniaxial, biaxial, and shear stress testing data of an elastomer sample similar to neoprene rubber [24]. A third-order Yeoh model is chosen to fit this data due to its ability to account for small and large strain values for incompressible materials while not being computationally expensive [24]. Non-linear least squares optimization is used during curve fitting to minimize error. Material constants C_{10} , C_{20} , and C_{30} are found from the strain energy equation W (1a) with I_1 (1b) as the first deviatoric strain invariant as a function of stretch ratios λ_i for $i=1,2,3$ (1c) or deformation of volume elements in the principal axes from deformed δ_i to undeformed lengths L_i :

$$W = C_{10}(I_1 - 3) + C_{20}(I_1 - 3)^2 + C_{30}(I_1 - 3)^3 \quad (1a)$$

$$\text{where } I_1 = \lambda_1^2 + \lambda_2^2 + \lambda_3^2 \text{ and } \lambda_i = \frac{\delta_i}{L_i} \quad (1b, c)$$

Curve fitting (Fig. 5) was used on test data in ANSYS for the following stress-strain equations (2), for uniaxial (σ_u), biaxial (σ_b), and shear (σ_s) as a function of a generalized strain variable λ substituted for known stretch ratios extension direction [25]:

$$\begin{bmatrix} \sigma_u \\ \sigma_b \\ \sigma_s \end{bmatrix} = 2 \begin{bmatrix} \left(\lambda - \frac{1}{\lambda^2} \right) \frac{\partial W}{\partial I_1} \\ \left(\lambda - \frac{1}{\lambda^5} \right) \frac{\partial W}{\partial I_1} \\ \left(\lambda - \frac{1}{\lambda^3} \right) \frac{\partial W}{\partial I_1} \end{bmatrix} \quad (2)$$

III. RESULTS AND DISCUSSION

Inputting the required material considerations, geometry, and boundary and loading conditions, the deformation of the compliant mechanism was simulated in ANSYS to find its kinematics relationship to thumb rotation and MCPH translation, and results were plotted in MATLAB.

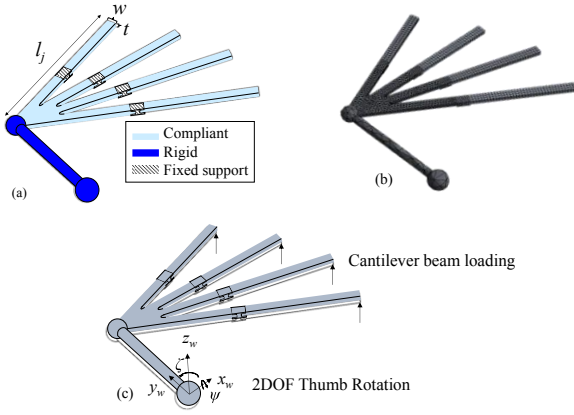


Fig. 4 FEM model set up (a) Defining the materials and boundary conditions. (b) Generating the mesh. (c) Applying the loads.

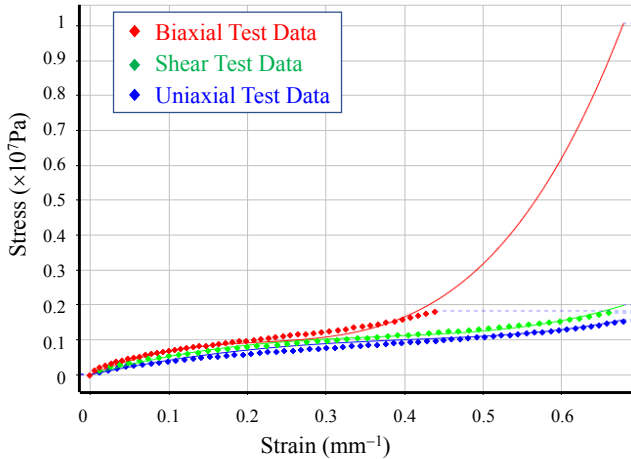


Fig. 5. Curve fitting to test data in ANSYS for an elastomer.

A. Simulation Results

Total deformation in each axis was captured to observe the evolution of the grasping configuration. Thumb rotation ranged from $0 \leq \zeta \leq 15^\circ$ and $0 \leq \psi \leq 15^\circ$, and simulation results were obtained at every 5° . Buckling behavior is observed in the area of the palm directly connected to the thumb linkage which creates a convex surface. Alternatively, the individual bending of cantilever compliant beam forms a concave contacting surface. If, for example, the rigid object to be grasped is a sphere, the palm can be assumed to not fully conform to the surface with a constant radius of curvature. For objects of diverse geometries and sizes this can prove beneficial to understand the appropriate application of this mechanism and the distinct contacting regions that may occur. Taking discrete points along the neutral axis of each beam, the compliant structure's

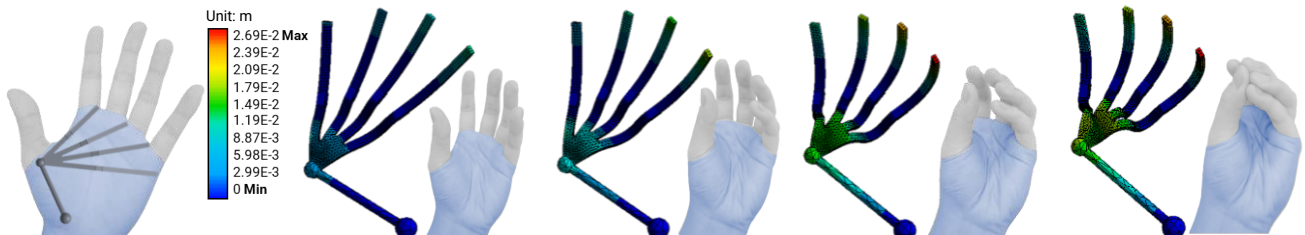


Fig. 6 FEM results with associated hand poses stepping from a flat palm configuration to the fully deformed state for a fully rotated thumb

deformation from the FEM was plotted in the case of maximum thumb rotation (Fig. 7). Observing the x - z planar view of the 3D plot in MATLAB, the varied concavity of the palmar region is observed, which for future applications for demonstrating object grasping can be useful to predict level of conformity that may require contact at multiple points along its surface. Collectively, when observing the side by side comparison with the hand poses with performing thumb opposition in a pinch-like grasping configuration from the initial flat palm state, this demonstrates the ability for CAPM to mimic shaping of the palm when simplified to two sets of rotational and transitional joints acting on a single compliant mechanism.

B. Kinematics Study

For the case of thumb rotation in between the flat palm configuration and the fully rotated thumb during opposition, the neutral axis of the $j = 4^{\text{th}}$ beam was plotted to observe the forward kinematics relationship between the rotational angles and the movable surface (Fig. 8).

The fixed midpoint of the palmar mechanism imposes the rightmost boundary condition of no deformation and the opposite end converges to the thumb MCPH which can be modeled simply as the location of the thumb linkage when rotated in two degrees. When changing the angle of rotation in ζ and ψ by 5° and observing its effect on the shaping of the hyperelastic structure, multi-modal buckling behavior is exhibited, especially in the case where $\zeta > \psi$. While the deformation for this complex geometry is unpredictable and difficult to model analytically, FEM provides a tool to find discrete solutions of the forward model to give information regarding the potential shaping of the palm rather than assume no prior knowledge on the effect a large, soft surface has before and after grasping. This can provide insight when performing a task on which configuration of the palm is best, and the anticipated joint angles to create this ideal setup.

IV. CONCLUSION

To design a multi-purpose robotic hand that can perform a variety of tasks requiring interchangeability between precision and power grasps, an anatomically inspired design methodology is used to understand the fundamental behavior of which parameters drive palmar deformation relative to the fingers. A complex biological system is simplified to defining kinematics for a compliant structure driven by a 2DOF rotational thumb and translational MCPH joints at the free end of cantilever beams. Designed to minimize the number of parts, CAPM is modeled as a geometrically complex, hyperelastic structure in FEM as a non-linear problem to simulate shaping similar to the human hand.

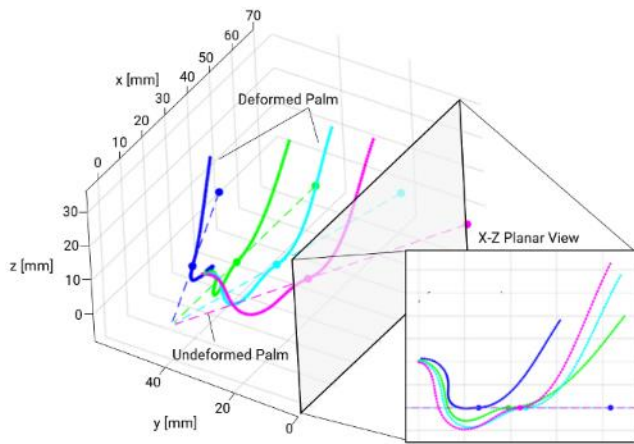


Fig. 7 Plotting beam neutral axis deformation for a fully rotated thumb.

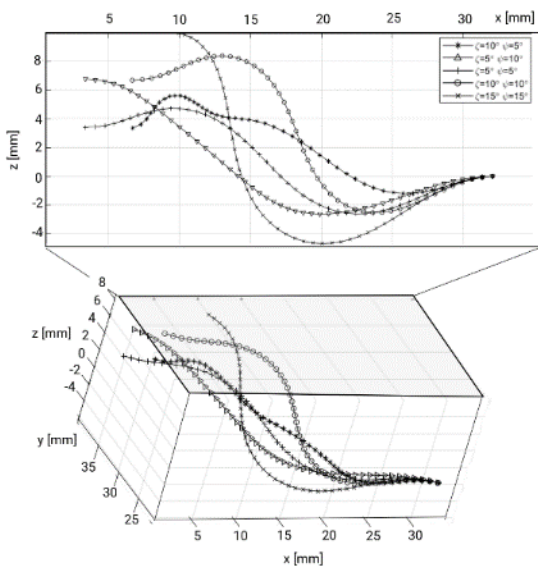


Fig. 8 Varying thumb rotation angles to plot $j=4$ beam neutral axis deformation.

REFERENCES

- [1] J. Rosmarin, H. Asada, "Synergistic Design of a Humanoid Hand with Hybrid DC Motor - SMA Array Actuators Embedded in the Palm." *IEEE Int. Conf. on Robotics and Automation*, pp. 773-778, 2008.
- [2] H. Liu, K. Wu, P. Meusel, N. Seitz, G. Hirzinger, M. Jin, Z. Chen, "Multisensory Five-Finger Dexterous Hand: The DLR/HIT Hand II." *IEEE/RSJ Int. Conf. on Intelligent Robots and System*, pp. 3692-3697, 2008.
- [3] M. Carozza, G. Cappiello, G. Stellin, F. Zaccone, F. Vecchi, S. Micera, P. Dario, "On the Development of a Novel Adaptive Prosthetic Hand with Compliant Joints: Experimental Platform and EMG Control." *IEEE/RSJ International Conference on Intelligent Robots and Systems*. pp. 1271-1276, 2005.
- [4] J. Meng, L. Gerez, J. Chapman, M. Liarakapis, M. "A Tendon-Driven, Preloaded, Pneumatically Actuated, Soft Robotic Gripper with a Telescopic Palm." *IEEE Int. Conf. on Soft Robotics (RoboSoft)*. pp. 476-481, 2020.
- [5] J. Zhou, X. Chen, U. Chang, J. Lu, C. Leung, Y. Chen *et al.*, "A Soft-Robotic Approach to Anthropomorphic Robotic Hand Dexterity." *IEEE Access*, vol. 7, pp. 101483-101495, 2019.
- [6] R. Deimel, O. Brock, "A Novel Type of Compliant, Underactuated Robotic Hand for Dexterous Grasping." *Robotics: Science and Systems X*, vol. 35, no. 1-3, pp. 161-185, 2014.
- [7] G. Wei, J. Dai, S. Wang, H. Luo, J. Craig *et al.*, "Kinematic Analysis and Prototype of a Metamorphic Anthropomorphic Hand with a Reconfigurable Palm." *Int. J. of Humanoid Robotics*, pp. 459-479, 2011.
- [8] D. Aukes, S. Kim, P. Garcia, A. Edsinger, M. Cutkosky, "Selectively Compliant Underactuated Hand for Mobile Manipulation." *IEEE Int. Conf. on Robotics and Automation*, pp. 2824-2829, 2012.
- [9] P. Morales, G. Grioli, C. Piazza, A. Bicchi, M. Catalano, "Exploring the Role of Palm Concavity and Adaptability in Soft Synergistic Robotic Hands." *IEEE Robotics and Automation Letters*, vol. 5, no. 3, pp. 4703-4710, 2020.
- [10] A. Pagoli, F. Chapelle, J. Corrales, Y. Mezouar, Y. Lapusta, "A Soft Robotic Gripper with an Active Palm and Reconfigurable Fingers for Fully Dexterous In-Hand Manipulation." *IEEE Robotics and Automation Letters*, vol. 6, no. 4, pp. 7706-7713, 2021.
- [11] J. Rossi, E. Berton, L. Grélot, B. Charlie, L. Vigouroux, "Characterization of Forces Exerted by the Entire Hand during the Power Grip: Effect of the Handle Diameter," *Ergonomics*, vol. 55, no. 6, pp. 682-692, 2012.
- [12] S. Heo, C. Kim, T. Kim, H. Park, "Human-Palm-Inspired Artificial Skin Material Enhances Operational Functionality of Hand Manipulation." *Advanced Functional Materials*, vol. 30, no. 25, 2020.
- [13] Y. Li, Y. Wei, Y. Yang, Y. Chen, "A Novel Versatile Robotic Palm Inspired by Human Hand." *Engineering Research Express*, 1(1), 015008, 2019.
- [14] R. Deimel, O. Brock, "A Compliant Hand based on a Novel Pneumatic Actuator." *IEEE Int. Conf. on Robotics and Automation*, pp. 2047-2053, 2013.
- [15] J. Zhou, S. Chen, Z. Wang, "A Soft-Robotic Gripper with Enhanced Object Adaptation and Grasping Reliability." *IEEE Robotics and Automation Letters*, vol. 2, no. 4, pp. 2287-2293, 2017.
- [16] R. Ansola, E. Veguería, A. Maturana, J. Canales, J. "3D Compliant Mechanisms Synthesis by a Finite Element Addition Procedure." *Finite Elements in Analysis and Design*, vol. 46, no. 9, pp. 760-769, 2010.
- [17] M. Cutkosky, "On Grasp Choice, Grasp Models, and the Design of Hands for Manufacturing Tasks." *IEEE Trans. on Robotics and Automation*, 5(3), pp. 269-279, 1989.
- [18] T. Feix, J. Romero, H. Schmiebmayer, A. Dollar, M. Kragic, "The GRASP Taxonomy of Human Grasp Types," *IEEE Trans. on Human-Machine Systems*, vol. 46, no. 1, pp. 66-77, 2016.
- [19] J. Landsmeer, "Power Grip and Precision Handling," *Ann. Rheum. Dis.*, vol. 21, pp. 164-170, 1962.
- [20] J. Napier, "The Prehensile Movements of the Human Hand." *The Journal of Bone and Joint Surgery*, British Volume, 38-B(4), pp. 902-913, 1956
- [21] I. Kapandji, "The Physiology of the Joints Upper Limb Volume I. Second Edition", *British J. of Surgery*, vol. 57, no. 8, pp. 168-175, 1970.
- [22] A. Sangole, M. Levin, "Arches of the Hand in Reach to Grasp." *Journal of Biomechanics*, vol. 41, no. 4, pp. 829-837, 2008.
- [23] A. Toro-Ossaba, J. Tejada, S. Rúa, A. López-González, "A Proposal of Bioinspired Soft Active Hand Prosthesis." *Biomimetics*, 8(1):29, 2023.
- [24] K. Miller, "Testing Elastomers for Hyperelastic Material Models in Finite Element Analysis," <https://www.axelproducts.com/downloads/FirstLoad.pdf>, 2017
- [25] O. Yeoh, "Some forms of the strain energy function for rubber," *Rubber Chemistry and technology*, vol. 66, no. 5, pp. 754-771, 1993.